Non-target LC-HRMS to Study the Exposome of Mild Cognitive Impairment and Alzheimer's Disease on Cerebrospinal Fluid

Begoña Talavera Andújar[1*], *Arnaud Mary*[1], *Tiejun Cheng*[2], *Leonid Zaslavsky*[2], *Evan E. Bolton*[2], *Michael T. Heneka*[1], *Emma L. Schymanski*[1*]

1. Luxembourg Centre for Systems Biomedicine (LCSB), University of Luxembourg, Avenue du Swing 6, L-4367 Belvaux, Luxembourg

2. National Center for Biotechnology Information, National Library of Medicine, National Institutes of Health, Bethesda, MD 20894, USA

ORCIDs: BTA: 0000-0002-3430-9255, AM: 0000-0002-6597-766X, TC: 0000-0002-4486-3356, LZ: 0000-0001-5873-4873, EEB: 0000-0002-5959-6190, MTH: 0000-0003-4996-1630, ELS: 0000-0001-6868-8145

ABSTRACT

Alzheimer's Disease (AD) is a complex and multifactorial neurodegenerative disease. The current diagnosis relies on non-specific biomarkers ($A\beta_{1\text{-}42}$, t-Tau, and p-Tau) measured in cerebrospinal fluid (CSF), which do not provide sufficient insights into disease progression. Studying the exposome could reveal new disease-specific biomarkers for more accurate diagnosis. In this pilot study, exposomics was performed on the CSF of three groups; AD, Mild Cognitive Impairment (MCI) due to AD, and a non-demented control group (ND), using non-target high resolution mass spectrometry (NT-HRMS) coupled with liquid chromatography (LC). An open-source cheminformatics pipeline was developed using MS-DIAL and patRoon with PubChemLite for Exposomics, plus CSF- and AD-specific suspect lists. Fifteen statistically significant chemicals (nine Level l, six Level 2a) from diverse classes (amino acids, gut metabolites, sugars, environmental chemicals) were identified. Most of the relevant chemicals (thirteen out of fifteen) were detected using the Hydrophilic Interaction LC (HILIC) method. Environmental and lifestyle factors may explain some chemical differences found across groups, such as the higher levels of indole-3-acetic acid found in the AD and MCI compared to the ND group. This work provides a strong methodological basis and several promising hypotheses to upscale these efforts on larger AD cohort numbers in future studies.

GRAPHICAL ABSTRACT`

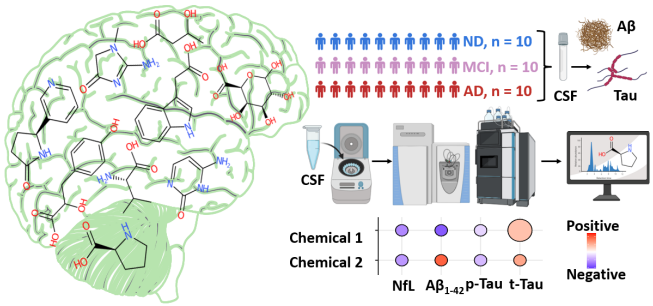

KEYWORDS: High resolution mass spectrometry, liquid chromatography, exposomics, cheminformatics, cerebrospinal fluid, Alzheimer's disease

INTRODUCTION

Alzheimer's Disease (AD) is a complex and multifactorial neurodegenerative disease where genetics, lifestyle and environmental factors may influence the pathogenesis. AD is the most common form of dementia, and its prevalence is expected to increase from 50 million people (2010) to 113 million by 2050 worldwide[1,2]. AD is often divided into three stages: (1) preclinical stage characterized by normal cognitive ability, (2) prodromal stage characterized by mild cognitive impairment (MCI) and (3) dementia stage[1,3]. There is a growing evidence that neuroinflammation may play a fundamental role in the pathology of the disease[4,5]. Alterations in the gut microbiota composition (gut dysbiosis) could change the gut barrier permeability and induce immune activation leading to systemic inflammation, which could alter the blood brain barrier (BBB) permeability, promoting neuroinflammation, and finally neurodegeneration associated to the formation of β-amyloid (Aβ) aggregates and tau neurofibrillary tangles. This can be explained by the bidirectional communication between the brain and the gut's microbiota, known as microbiota-gut-brain-axis (MGBA)[6,7].

The current diagnosis for AD is based on clinical symptoms and pathological alterations such as reduced $A\beta_{1\text{-}42}$ or increased p-Tau and t-Tau concentrations in cerebrospinal fluid (CSF). However, AD pathology starts decades before the clinical symptoms appear. Moreover, Aβ and tau protein are quite stable in clinical AD, and may not always differentiate AD from other forms of dementia, leading to a high rate of misdiagnosis in the early stages[7,8]. While elevated levels of neurofilament light (NfL) are also found in CSF of AD patients, this is also a nonspecific biomarker of degeneration since its levels are elevated in multiple neurodegenerative diseases[9]. Hence, research is urgently needed to find additional and specific biomarkers that could help in an early diagnosis and better understanding of the disease progression.

CSF is the closest biological fluid to the brain and abnormalities in this matrix are directly related to pathological changes in the brain. Since it is already collected for AD diagnosis, further investigation of its chemical composition (e.g., via metabolomics and exposomics) could provide new insights to better understand disease progression. To date the number of exposomics studies in CSF samples is still very low. However, several open resources exist to support exposomics of CSF, including the CSF Metabolome database[10,11], containing about 468 metabolites found in human CSF, and PubChemLite for Exposomics (PCL)[12], a subset of PubChem[13,14] designed to support efficient annotation in exposomics and metabolomics studies. Non-target high-resolution mass spectrometry (NT-HRMS) coupled to liquid chromatography (LC) is well suited to perform exposomics studies on CSF. Previous work focusing on Parkinson's disease (PD) using plasma and feces described an open source workflow including MS-DIAL, patRoon and PCL, complemented with disease-specific databases and suspect lists[15]. The current work extends this approach to develop suspect lists and databases relevant for AD and apply this to CSF analysis.

This study investigates the exposome and metabolome in the CSF of AD, MCI, and a non-demented control group (ND), meaning neurological patients without dementia and without central nervous system (CNS) neurodegeneration. The additional MCI group offers the opportunity to study disease progression. CSF was analyzed by NT-HRMS coupled to two different LC methods to explore potential associations between clinical AD biomarkers ($A\beta_{1\text{-}42}$, t-Tau, p-Tau and NfL) and chemicals identified in the samples. This pilot study was designed to establish methods and develop hypotheses to investigate in a larger cohort of patients in future studies.

MATERIALS AND METHODS

Human CSF sample collection

A total of 30 CSF human samples (n = 10/group) were extracted by lumbar puncture and stored at –80 °C until analysis. Informed consent was obtained (see Ethics Declaration). CSF biomarkers- $A\beta_{1\text{-}40}$, $A\beta_{1\text{-}42}$, t-Tau, p-Tau, and NfL- were measured with a Lumipulse G600II analyzer (Fujirebio). See Supporting Information (SI), **Section S1.1.**

Sample preparation

The sample preparation was adapted from Song et al.[16]. Briefly, CSF samples were mixed with ethanol, vortexed, incubated (-20°C) and centrifuged. The supernatant was evaporated to dryness and reconstituted using Milli-Q water:MeOH:MeCN (2:1:1, v/v/v). Four different pooled Quality Control (QC) samples were prepared following published recommendations[17,18] (see **S1.2**). The sample preparation method was first tested in artificial CSF (aCSF) samples (HelloBio Ltd, UK) using the same protocol as above, but also adding 10 µL of a polar chemical standard mixture to serve as reference standards later (see **S1.3)**.

Instrumental analysis

Non-target analysis was performed as described previously[15] on a Thermo Scientific Accela LC system coupled to a Q Exactive™ HF (Thermo Scientific) mass spectrometer (MS) using Electrospray Ionization (ESI) in both positive (+) and negative (-) modes. BEH C_{18} reversed phase (RP) and SeQuant® ZIC-pHILIC 5 µm polymer (HILIC) columns were used (in separate runs) to detect a broader range of chemicals.

Data processing

The raw files (".raw") were converted to ".mzML" using ProteoWizard MSConverter (Version 3.0.20331.3768aa6e9 64-bit)[19] and analyzed with MS-DIAL (version 4.90)[20], MS-FINDER (version 3.52)[21,22] and patRoon (version 2.1.0)[23,24]. MS-DIAL (using public libraries, see **Table S4**) combined with MS-FINDER was employed for non-target screening, while patRoon was used for both suspect and non-target screening (see **S1.4**). **Figure 1** shows the databases and suspect lists employed for each of the patRoon approaches; those marked with an asterisk were created in house to explore chemicals focused on AD and other related CNS diseases (see **S1.5,** GitLab[25] and Zenodo[26] repositories).

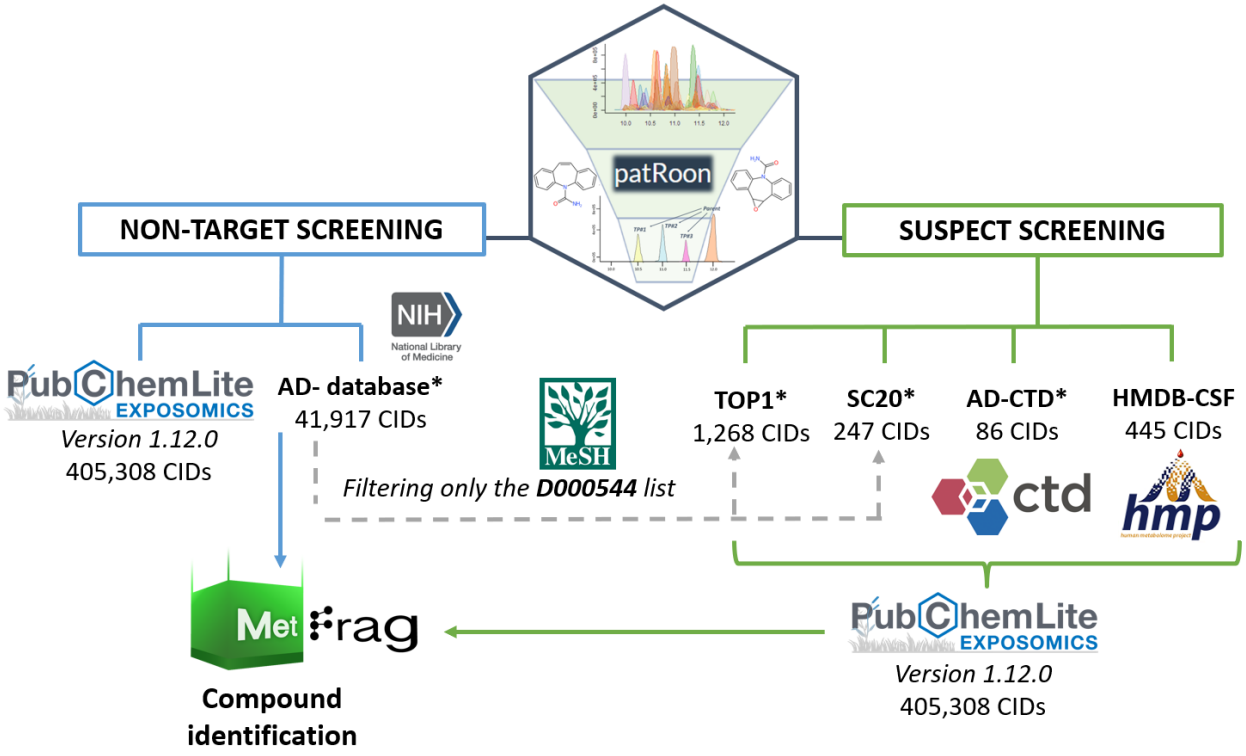

Figure 1. Databases and suspect lists employed for the non-target screening (left) and the suspect screening (right) analysis with patRoon. *Indicates databases/suspect lists created for the purpose of this study[25–27]. See **S1.5** and **Table S5** for more details.

Features were annotated based on the *individualMoNAscore* (0-1) for patRoon, *Dot product* (0-100) and *fragment presence* (0-100) for MS-DIAL, and MS-FINDER score (0-10), as previously described[15,28], with slight modifications for MS-DIAL and MS-FINDER (see **Table S6**). *OrgMassSpecR*[29–31] was used to calculate spectral similarity. Identifications were considered Level 1 when the match between the standard and tentative candidate (in the CSF) yielded a *SpectrumSimilarity* score ≥ 0.7 and the retention time (RT) shift was <1min. Xcalibur Qual Browser (version 4.1.31.9) was used to check the RT and to extract the MS/MS information. All codes are available online[25].

Statistical analysis

First, data was pre-processed with MetaboAnalyst 5.0[32,33] by filtering (interquartile range option), normalization by sum, log transformation (base 10), and pareto scaling. Then, R was used to compute one-way analysis of variance (ANOVA) with post-hoc Tukey's Honestly Significant Difference (HSD) test for multiple comparisons. Features with post-hoc test p-values < 0.05 were considered as statistically significant. Additionally, area under the receiver operating characteristic (ROC) curves (AUC) were computed (MetaboAnalyst 5.0). The chemical was considered an *excellent* classifier when AUC = 1.0-0.9, and *good* when AUC = 0.9-0.8, following published guidelines[34]. Finally, linear multiple regression analysis was used (via the *lm* function in R) to analyze the relationship between the biomarker concentrations ($A\beta_{1\text{-}40}$, $A\beta_{1\text{-}42}$, p-Tau, t-Tau and NfL) and the chemical features found in CSF (see **S1.6**).

RESULTS

Table 1 summarizes the statistically significant Level 1-2a features (p-value < 0.05) identified using at least one of the different approaches (software, database, or LC mode). The values from the method with the *best* peak intensities and/or p-values are presented in **Table 1** for simplicity. Full results are available in **Table S7-S14**. Considerable efforts were made to confirm the identities of the relevant chemicals, with finally nine out of the fifteen features confirmed via reference standard, i.e., Level 1. **S2.1** summarizes the identification workflow using the example cytosine (Level 2a).

Table 1. Statistically relevant features found by MS-DIAL and patRoon. Only Level 1 and Level 2a features are included. * Indicates p-value <0.05 as well as *good* or *excellent* biomarkers. (a) Mannose is grouped with its isomers glucose, galactose, and fructose as they are indistinguishable with the methods used (b) Neotame is a derivative of the IS Neotame-D_3. IL = Identification Level. "LC Mode" indicates the method that provided the best peak intensities and/ or p-value (see **Table S7-14** for detailed information).

					ANOVA	**Post-hoc test p-values**			**AUC curves (ROC analysis)**		
Chemical name	**mz**	**rt (min)**	**LC mode**	**IL**	**p-value**	**MCI-AD**	**ND-AD**	**ND-MCI**	**MCI-AD**	**ND-AD**	**ND-MCI**
Adenine	136.0617	3.42	HILIC (+)	1	0.0091*	0.9958	0.0213*	0.0174*	0.50	0.87*	0.80*
Creatinine	112.051	3.58	HILIC (-)	1	0.0146	0.9096	0.0482*	0.0189*	0.55	0.86*	0.81*
Diazepam	285.0787	17.11	RP (+)	2a	0.0447*	0.0373*	0.6052	0.2429	0.64	0.83*	0.5
Cytosine	112.0505	5.9	HILIC (+)	2a	0.0253*	0.0216*	0.6122	0.1575	0.78	0.69	0.71
Mannose (a)	179.0549	9.18	HILIC (-)	2a	0.0292*	0.7888	0.0292*	0.1164	0.52	0.91*	0.69
Threonic acid	135.0291	10.48	HILIC (-)	1	0.0457*	0.4707	0.3345	0.0361*	0.62	0.77	0.85*
Galacturonic acid	193.0342	12.24	HILIC (-)	1	0.0305*	0.9534	0.0753	0.0403*	0.54	0.79	0.83*
3-hydroxybutanoic acid (BHBA)	103.0396	5.92	HILIC (-)	1	0.0030*	0.0042*	0.0150*	0.8637	0.89*	0.86*	0.59
Neotame (b)	377.2062	15.89	RP (-)	2a	0.0070*	0.0229*	0.9456	0.0108*	0.77	0.61	0.86*
Cotinine	177.1021	1.76	HILIC (+)	1	0.0284*	0.0916	0.8744	0.0320*	0.70	0.63	0.81*
N-Acetylhistidine	196.0717	8.15	HILIC (-)	2a	0.0102*	0.0348*	0.9193	0.0141*	0.81*	0.5	0.81*
4-Hydroxyphenyllactic acid (4-HPLA)	181.0495	6.46	HILIC (-)	2a	0.0285*	0.9935	0.0574	0.0455*	0.53	0.80*	0.83*
Indole-3-Acetic Acid (IAA)	176.0706	13.66	RP (+)	1	0.0234*	0.7237	0.1144	0.0221*	0.57	0.82*	0.81*
L-Valine	118.0862	6.99	HILIC (+)	1	0.0105*	0.9996	0.0224*	0.0211*	0.50	0.86*	0.84*
L-Proline	116.07	6.92	HILIC (+)	1	0.0280*	0.0569	0.9927	0.0444*	0.83*	0.55	0.82*

MS-DIAL identifications

A total number of 149 unique features were annotated as Level 1 and Level 2a with the RP (45 unique) and HILIC (61 unique) separation modes, with 43 features overlapping (InChIKeys were employed to deduplicate, see **S2.2**). **Figure 2** shows the *m/z* and intensity of all the tentative candidates identified with MS-DIAL and MS-FINDER. The high confidence features (Level 1-2a), consisting primarily of small molecules, generally exhibit higher peak intensities, while Level 5 features are more diverse, from low to high masses, and the peak intensities are mainly low (**Table S7**).

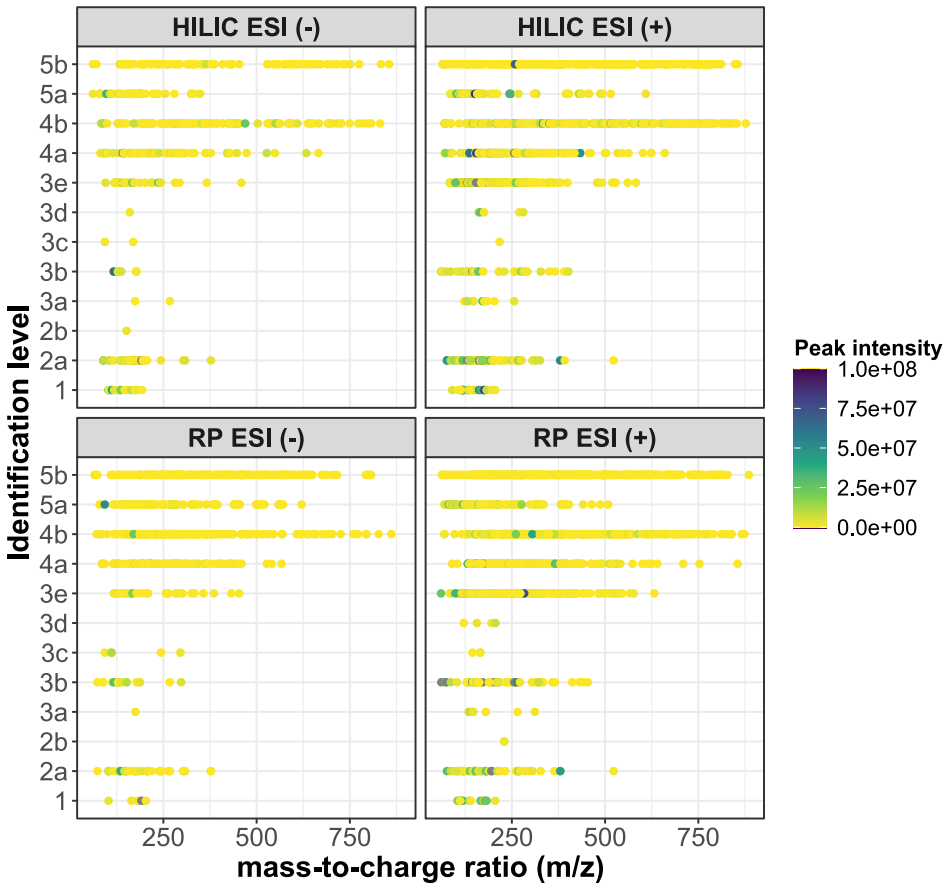

Figure 2. Dot plot showing the *m/z* distribution of the tentative annotated features, shaded according to peak intensity. Each dot represents the maximum peak intensity found in the samples. Level 1 features are confirmed by reference standard while Level 2a are based on scores. See **Table S6** for detailed information about the ILs.

After performing the ANOVA post-hoc tests, 95, 111, and 571 features were identified as statistically relevant (p- value < 0.05) in the MCI-AD, AD-ND, and ND-MCI groups, respectively (**Table S8**). Nevertheless, only twenty features were within the high confidence range (Levels 1-2a) and only twelve features were unique (first twelve rows of **Table 1**), as some chemicals were identified as statistically relevant by more than one LC and ionization method (e.g., adenine and cotinine were identified as relevant by both RP and HILIC). All the statistically relevant chemicals, except for cytosine, were classified as *good* or *excellent* classifiers.

patRoon identifications

Non-target screening

There were 17 and 23 unique features annotated by RP and HILIC, respectively using patRoon non-target screening approach with the PCL database. The same features were identified with the AD-database except for metoprolol acid (Level 2a), L-beta-homolysine (Level 3a) and neotame (Level 2a). The presence of neotame was later confirmed to be as a derivative of the IS, neotame-D_3, employed to check the instrument performance (see **S2.3** and **Table S9-S10**). Although only 18,677 chemicals overlap between the PCL and AD-database, most of the features found in the CSF samples were within this overlap, even though PCL has many more chemicals. This implies that the AD-database provides adequate coverage, as similar results were obtained with fewer entries in the database, which ultimately led to a faster (more efficient) data analysis.

After computing the post-hoc ANOVA tests, four features were found to be statistically significant using PCL. The same features were found as relevant with the AD-database except for L-proline (**Table S11-S12**). Three of them were confirmed with the reference standard, (Indole-3-Acetic Acid (IAA), L-valine and L-proline), last three rows of **Table 1**, whilst the other was annotated as Level 3a (quinoline).

Suspect screening

Figure 3 illustrates the number of annotated features and overlapping in each of the different suspect lists **(A)** as well as the identification levels of each of the features **(B),** separated by HILIC (+ and -); RP results are in **S2.4**. Of the four suspect lists used, most of the unique features were found in the largest lists: TOP1 and HMDB-CSF. Overall, the overlap between the suspect lists was low. Interestingly, the HILIC LC method showed a considerably higher number of unique features in the HMDB-CSF suspect list, suggesting that this might be a better chromatographic approach for the CSF analysis, due to the polarity of the matrix. Additionally, more Level 1 features were found using HILIC rather than RP (**Table S13**).

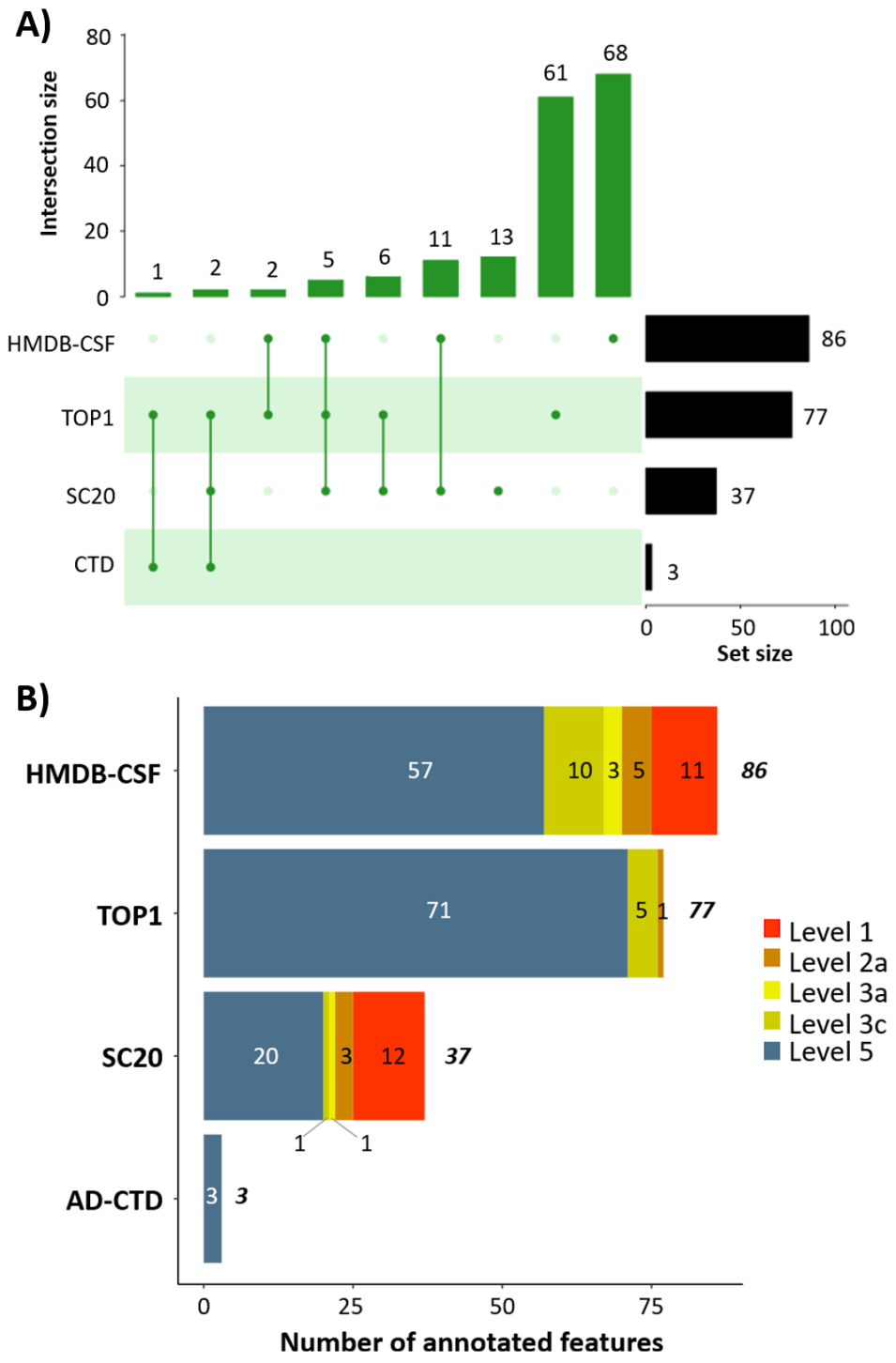

223

224 **Figure 3.** (A) UpSet plot representing the number of annotated features in each suspect list plus
225 the overlap across lists. (B) Bar plots showing the identification levels of the annotated features in
226 each suspect list. Features identified by positive and negative ionization modes were combined in
227 these plots for simplicity, only HILIC results are shown - see **S2.4**, **Figure S11**, for RP. See **S1.5**
228 for detailed information about the suspect lists.
229

Fifteen statistically relevant features were found by the different suspect screening approaches (**Table S14**). Most of the statistically relevant chemicals (thirteen) were found with the TOP1 suspect list, all classified as Level 5. One Level 1 chemical was identified with HMDB-CSF and SC20, L-proline, displayed in **Table 1**, while one Level 3c feature (N-acetylaspartylglutamic acid) was annotated using the HMDB-CSF list (see **S2.4**, **Figure S12).**

DISCUSSION

This discussion focusses on the statistically significant Level 1 and 2a chemicals (**Table 1**) since most of the low confidence features exhibited low peak intensities (**Figure 2**). The discussion is divided by chemical classes, with major examples shown in **Figure 4**, before exploring the relationship between the CSF biomarkers ($A\beta_{1\text{-}42}$, p-Tau, t-Tau and NfL) and the statistically relevant chemicals found across the groups.

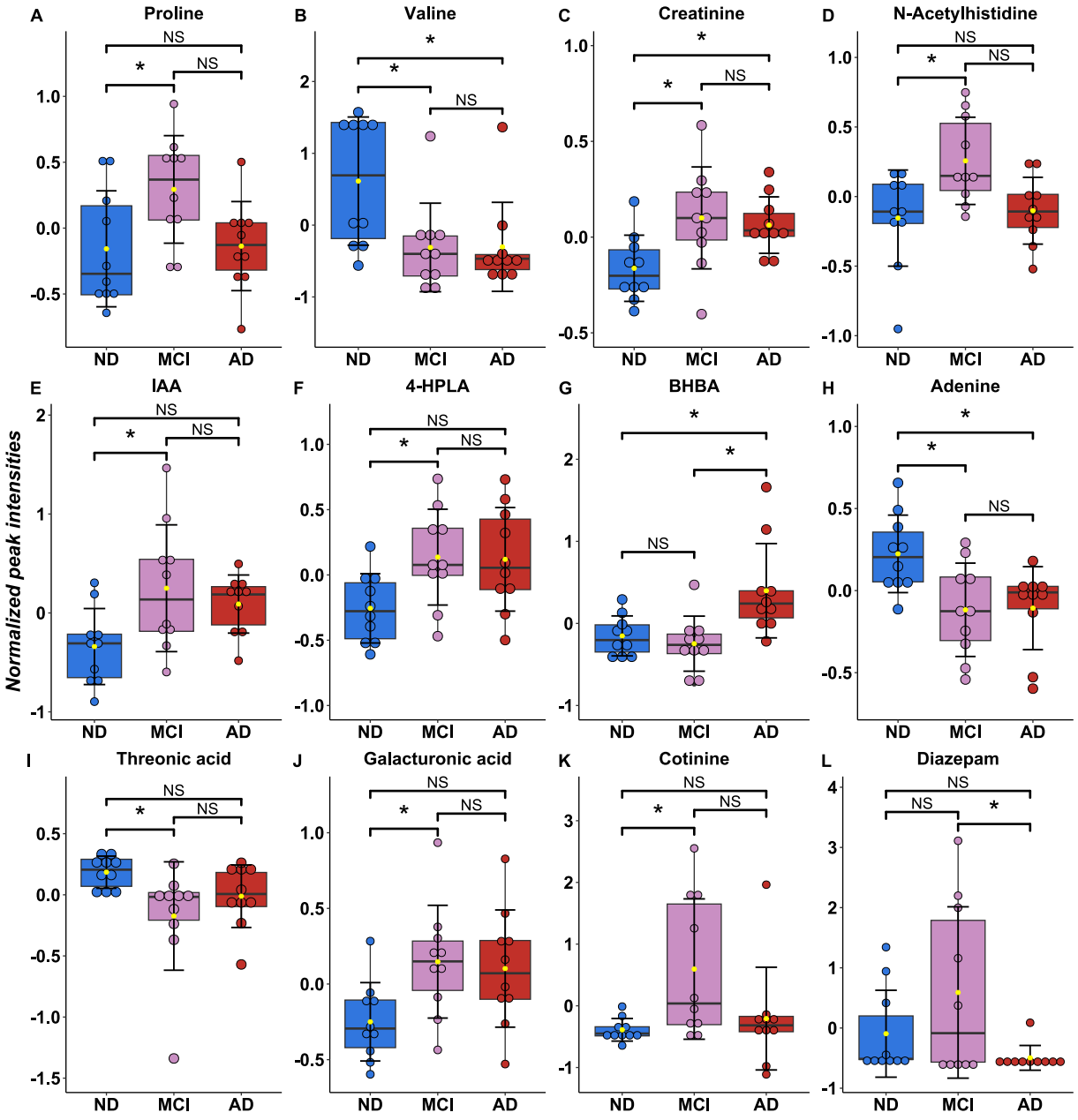

Figure 4. Bar plots showing the normalized peak intensities across groups of proline (A), valine (B), creatinine (C), N-Acetylhistidine (D), IAA (E), 4-HPLA (F), BHBA (G), adenine (H), threonic acid (I), galacturonic acid (J), cotinine (K) and diazepam (L). *: p-value <0.05, NS: Not Significant differences.

Amino acids and derivatives

Disrupted amino acids pathways were previously described[35–37] in AD and may be related to the alteration of different neurotransmitters. Here, higher levels of proline were found in the MCI group compared to the AD and ND groups (**Figure 4A**). Proline is a nonessential amino acid that was already identified as possible a biomarker of AD in CSF samples[35]. In addition, evidence has shown that proline metabolism is related to the ageing process and plays a key role in the progression from healthy to MCI and eventually to AD[36]. The results here are in line with these previous studies, since the higher levels found in the MCI group might suggest that this amino acid could be a biomarker of disease progression. Since proline is classified as a "*good"* biomarker (AUC > 0.8), it could help to discriminate between ND-MCI groups (see **S3.1**, **Figure S13**).

Valine showed statistically significant lower levels in the AD and MCI groups compared to the ND group, suggesting a progressive decrease in the disease (**Figure 4B**). Since AUC > 0.8 in the ND-MCI and ND-AD comparison, it may be a potential biomarker for disease progression. Decreased valine levels were already reported in AD, correlated to impaired neurotransmission and cognitive function[38]. This may be explained by the brain glucose hypometabolism in AD, which could lead to compensatory sources of energy, such as amino acids to form tricarboxylic acid cycle (TCA) intermediates[37].

Creatinine, an amino acid derivative, was found with statistically higher peak intensities in the AD and MCI groups compared to the ND group (**Figure 4C**), discriminating well between ND-AD and ND-MCI (AUC > 0.8). Higher levels of creatinine were noted previously in the CSF of AD, possibly due to multiple factors, including the excessive use of phosphocreatine as an energy source (followed by degradation to creatinine), disruptions in the creatinine-phosphocreatine

shuttle[37] and/or a compromised BBB integrity, allowing creatinine and other molecules to leak into CSF from blood [39].

Statistically higher levels of N-Acetylhistidine (Level 2a), a histidine derivative, were found in the MCI group compared to the AD and ND groups (**Figure 4D)**. Changes in this metabolite have been described in both AD[40] and PD[41], suggesting that the N-acetylation of amino acids may be affected in these neurological diseases.

Glutamate, lysine, histidine, arginine, glutamine, serine, and phenylalanine were found with lower levels in the AD group compared to the ND, without statistical relevance. This is consistent with previous works indicating metabolic alterations in AD[37,38]. Interestingly, some amino acids (lysine, arginine, tyrosine, and tryptophan) showed the highest levels in the MCI group (without statistical relevance), which may reflect the compensatory mechanisms in response to early neurodegenerative changes (see **S3.1**, **Figure S14)**.

Gut microbiota related metabolites

Statistically higher levels of indole-3-Acetic Acid (IAA) were found in the MCI group compared to ND, as well as in the AD group compared to ND (p-value = 0.1144, **Figure 4E**). IAA is an important microbial tryptophan metabolite which can modulate intestinal homeostasis and suppress inflammatory responses[42,43]. Here, IAA appears to be associated to cognitive impairment as described previously in serum samples from hemodialysis patients[44]. Statistically lower levels of the tyrosine metabolite, 4-hydroxyphenyllactic acid (4-HPLA), Level 2a, were found in the ND group compared to MCI (**Figure 4F**). This metabolite can be produced by *Lactobacillus sp.,* as previously reported[45]. Changes in 4-HPLA were previously described in AD[46]. Both IAA and 4-HPLA effectively discriminated MCI and AD, with AUC > 0.8. Changes in the gut microbiota composition and the onset of gastrointestinal symptoms are frequently observed in AD. A decrease

296 in the gut microbiota diversity has been reported in diagnosed patients[7,47] and this might be behind
297 the alterations in the CSF metabolites identified here.

298 The chemical 3-hydroxybutanoic acid, also known as β-hydroxybutyrate (BHBA), was detected
299 with statistically higher levels in the AD group compared to the MCI and ND groups (**Figure 4G**).
300 With an AUC > 0.8 it can be considered a "*good"* classifier. BHBA is the most abundant ketone
301 in the human circulation, can be an effective alternative energy substrate for the neurons, and may
302 be involved in many brain functions (neurotransmission, neuroinflammation and myelination). It
303 is possible that the higher levels found in the AD group were due to increased fat degradation and
304 thus ketone formation, including BHBA, as physiological response to the energy shortage in the
305 brain[48]. However, BHBA has been proposed as a promising therapeutic strategy for AD, as lower
306 levels were found previously[49]. This is support by evidence indicating that BHBA might inhibit
307 the NLRP3 inflammasome activation in human monocyte, reducing the neuroinflammation, hence
308 decreasing the AD pathology[49,50]. Nevertheless, although the liver is the primary source of BHBA,
309 it has been proven that gut microbiota could induce changes in its metabolism[51]. Moreover,
310 ketogenic diets, which elevate BHBA concentrations, may contribute to the higher levels observed
311 in the AD group. Multiple factors might explain the BHBA levels found here, such that further
312 research is needed to clarify the mechanisms in which BHBA participates in AD pathology (see
313 **S3.2**).

314 **Nucleobases**

315 Adenine (**Figure 4H**), a purine nucleobase, was found with statistically higher levels in the ND
316 group compared to the AD and MCI groups, as a "*good"* classifier. These results are consistent
317 with previous studies performed in mice[52], indicating that the purine metabolism pathway may be
318 altered in AD and potentially play an important role in the pathogenesis. Additionally, cytosine

(Level 2a) was found to be altered. This was also reported in urine samples[53], suggesting that the pyrimidine metabolism may be altered in AD[54] (see **S3.3**).

Sugars and sugar acids

Lower levels of threonic acid (**Figure 4I**) were found in the MCI group compared to ND. The same trend was observed between the AD and ND. Threonic acid reductions were observed in AD mice models[55], and oral administration of threonic acid prevented memory decline[56]. In contrast, lower levels of monosaccharides (e.g., mannose) were found in the AD group (see **S3.4**). Changes in both monosaccharides and threonic acid, were previously reported in CSF samples of PD[57]. Additionally, galacturonic acid (**Figure 4J**), was found with statistically lower levels in the ND group compared to MCI, as well as ND compared to AD. Galacturonic acid is the major component of pectin, a polysaccharide found in fruits and vegetables, so this could also be an environmental and lifestyle chemical where e.g. the higher levels found in both AD and MCI compared to the ND group could be due to the major BBB permeability, associated to the dementia status. Hence, this could be either a biomarker or BBB dysfunction. Pectins have been shown to impact the gut microbiota, since different bacterial species can break down the pectins and provide them as nutrients for other microbes[58].

Environmental and lifestyle chemicals

Significantly higher levels of cotinine (**Figure 4K**), the main metabolite of nicotine, were found in the MCI group compared to ND. The same trend was observed between the MCI and AD group. Interestingly, tobacco smoking has been correlated with a lower incidence of AD. Cotinine has shown to prevent memory loss and inhibit Aβ aggregation without the toxicity and addictive properties of its precursor (nicotine)[59,60]. Furthermore, diazepam (Level 2a), popularly known as "valium", was identified with statistically higher levels in the MCI group compared to the AD.

The same trend was observed between the MCI-and ND groups (**Figure 4L)**. Cotinine and diazepam could be considered lifestyle indicators.

Clinical associations between the altered chemicals

Figure 5 illustrates the associations between the chemicals discussed previously and the concentrations of CSF biomarkers in AD. While age, sex and $A\beta_{1\text{-}40}$ concentrations were considered as covariates to compute the different linear models, they are excluded for simplicity. Moreover, although female sex may be a risk factor for AD, sex differences are not discussed here due to the limited sample size, as well as the unbalanced number of women and men in each group. Although positive β-coefficient indicates a positive association between two variables (e.g., t-Tau concentrations and valine levels), an association does not necessarily imply causation.

Briefly, this analysis showed a significant positive association between valine and t-Tau concentrations in the AD group (top right of **Figure 5**), while the other groups presented negative association. In contrast, valine was negatively associated with CSF $A\beta_{1\text{-}42}$ concentrations (but without statistical significance). This is in line with a previous work showing that several amino acids were negatively correlated with $A\beta_{1\text{-}42}$[37]. Indeed, proline was also negatively correlated with $A\beta_{1\text{-}42}$ although it was not a significant association. Positive and significant associations between BHBA with NfL and p-Tau were found in the AD group, while a relevant negative association was found for t-Tau. Notably, one AD patient exhibited high outlier levels for NfL, BHBA, galacturonic acid and cotinine compared with the other patients in the group (see **S3.5**). Thus, it would be interesting to investigate in a future study whether the associations found here are due to the AD pathology or to environmental factors such as a ketogenic diet, as previously discussed. Finally, in the ND group, significant positive associations were found between adenine and NfL, and negative associations between adenine and t-Tau. This last association might suggest a

potential role of adenine in decreasing tau accumulation. The same trends were observed in the AD group, while opposite associations were noted in the MCI group. These contrasting associations in the MCI could suggest potential alterations in disease progression or underlying pathophysiological mechanisms specific to the MCI stage, which would have to be investigated further in future studies.

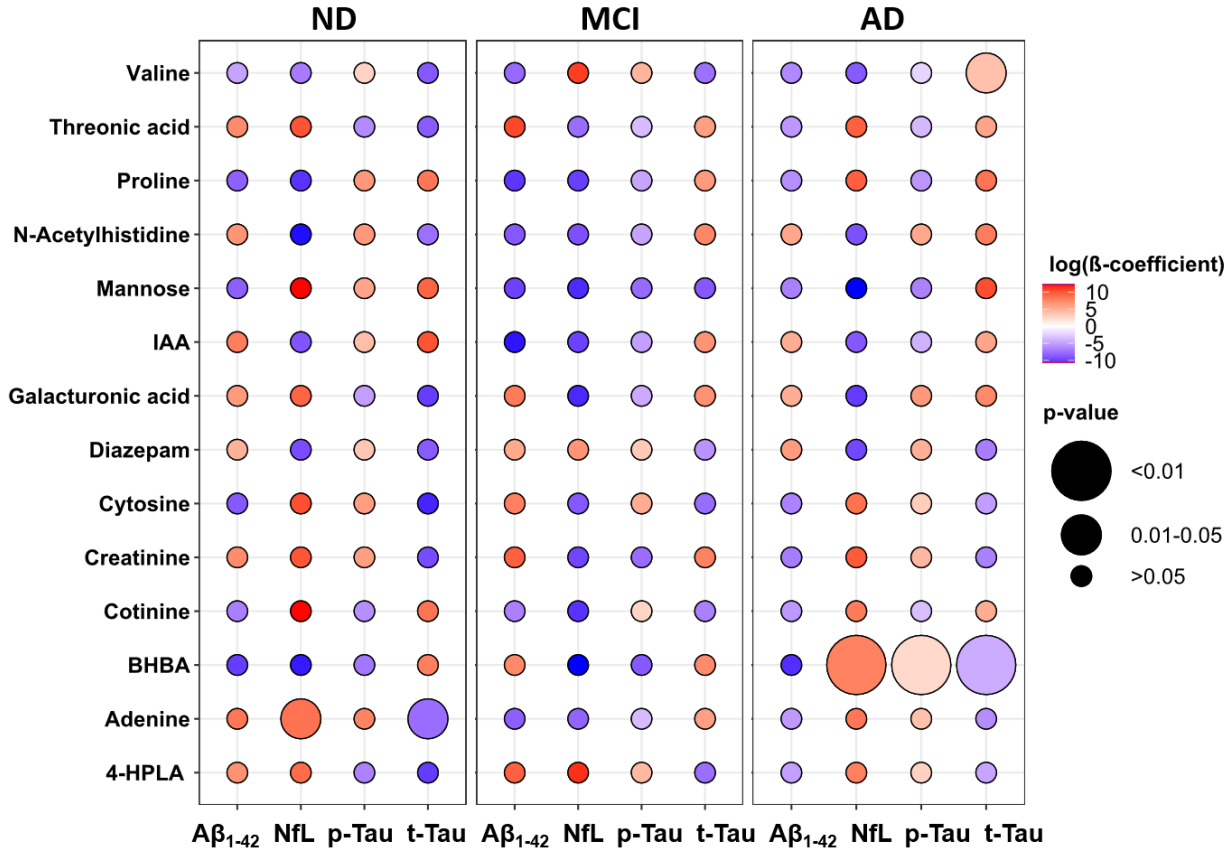

Figure 5. Associations between the statistically relevant chemicals (**Table 1**) and the CSF $A\beta_{1-42}$, NfL, t-Tau and p-Tau concentrations for the ND, MCI, and AD groups. Color represents the log transformed β-coefficients. Positive and negative associations are indicated by the red and blue colors, respectively. See **Table S15-17** for further details.

Future Perspectives

This study showed different chemical alterations in the CSF of AD, MCI, and ND groups. In contrast to a previous metabolomics study on AD[37], here a third group (MCI) was included to explore potential biomarkers of disease progression. Statistically higher levels of some chemicals (proline, creatinine, N-acetylhistidine, IAA, 4-HPLA, cotinine and diazepam) were observed in the MCI group compared to the others (see **Figure 4**). Most of the relevant chemicals were identified using the HILIC LC method (**Table 1**), which appears to be the most suitable method for future experiments. Overall, MS-DIAL provided a higher number of annotated chemicals; nevertheless, the combination of different software (MS-DIAL and patRoon), databases and suspect lists allowed the identification of different types of chemicals, increasing the overall understanding of the CSF metabolome/exposome. The AD-database was an efficient approach to screen for relevant chemicals in AD samples compared with PCL, as similar results were obtained with a ~10x smaller database, requiring less time for data analysis. This is consistent with our previous work[15] where the PD-specific database and PCL showed very similar results. Interestingly, the cooccurrence score of the annotated features varied widely (from low to high), indicating that this may not be a suitable metric to pre-select relevant entries (see **S3.6**). However, the exact mass of detected chemicals was within the range of 75 to 500 Da, such that exact mass filtering could reduce the database size further (32,109 entries between 75 and 500, compared with 41,917 unfiltered), and consequently, the analysis time. Level 1-2a chemicals detected here (e.g. galacturonic acid, threonic acid, N-acetylhistidine and diazepam) could help expand the current human CSF database, as they are not yet included). Environmental and lifestyle factors may explain some chemical differences found across the different groups as these factors may influence the composition and metabolic activity of the human microbiota, resulting in altered levels of some

metabolites (e.g., IAA). This highlights the possible role of the microbiota-gut-brain-axis (MGBA) in AD (see **S3.2**). This pilot study aims to establish methodologies and hypotheses that can be examined and validated in future studies involving a larger patient cohort and potentially other type of matrices (such as plasma or feces), which will help improve understanding of the underlying biological mechanisms and roles the chemicals and potential biomarkers identified here may have on AD progression.

ASSOCIATED CONTENT

Supporting Information.

The following files are available free of charge on the ACS Publication website and via DOI.

A Word file contains figures and additional details regarding material and methods (**S1**), results (**S2**) and discussion (**S3**). **Figures S1-S19** as well as **Table S1-1** can be found in this document.

An Excel file contains supplementary tables: **Tables S1-S17**.

The code functions, and files associated with this manuscript are provided in the ECI GitLab repository[25] (https://gitlab.lcsb.uni.lu/eci/AD-CSF). The PCL database and database/suspect lists used are available for download on Zenodo[26,27] (https://doi.org/10.5281/zenodo.8014420).

AUTHOR INFORMATION

Corresponding Author

*Email: begona.talavera@uni.lu and emma.schymanski@uni.lu

Author Contributions

BTA: conceptualization, data curation, formal analysis, investigation, methodology, software, validation, visualization, writing – original draft (lead), reviewing and editing. AM: formal analysis, investigation, writing- review and editing; TC: methodology, software, writing - review and editing; LZ: methodology, software, writing – review and editing; EEB: conceptualization, resources, software, supervision, writing – reviewing and editing; MTH: conceptualization, funding acquisition, resources, supervision, writing – reviewing and editing; ELS: conceptualization, data curation, resources, software, supervision, writing – original draft (supporting), writing – review and editing.

Ethics declarations

Informed consent for use of samples and data for research purposes was given with the local ethics committee approval (University Hospital of Bonn Ethics Commission #279/10). This work does not contain identifiable data of the subjects or any other specific individual person's data.

Funding Sources

BTA is part of the "Microbiomes in One Health" PhD training program, which is supported by the PRIDE doctoral research funding scheme (PRIDE/11823097) of the Luxembourg National Research Fund (FNR). The work of EEB, TC, and LZ was supported by the National Center for Biotechnology Information of the National Library of Medicine (NLM), National Institutes of Health. ELS acknowledges funding support from the FNR for project A18/BM/12341006, MTH acknowledges funding support from the FNR within the PEARL programme (FNR/16745220).

ACKNOWLEDGMENT

BTA acknowledges support from Gianfranco Frigerio during sample preparation and advice from Corey Griffith and Lorenzo Favilli during data processing/interpretation. We thank the Metabolomics Platform of the LCSB for their support with the LC-HRMS analysis and other Environmental Cheminformatics and PubChem team members who contributed to this work indirectly via other collaborative and scientific activities.

REFERENCES

(1) Knopman, D. S.; Amieva, H.; Petersen, R. C.; Chételat, G.; Holtzman, D. M.; Hyman, B. T.; Nixon, R. A.; Jones, D. T. Alzheimer Disease. *Nat Rev Dis Primers* **2021**, *7* (1), 1–21. https://doi.org/10.1038/s41572-021-00269-y.

(2) Reveglia, P.; Paolillo, C.; Ferretti, G.; De Carlo, A.; Angiolillo, A.; Nasso, R.; Caputo, M.; Matrone, C.; Di Costanzo, A.; Corso, G. Challenges in LC–MS-Based Metabolomics for Alzheimer's Disease Early Detection: Targeted Approaches versus Untargeted Approaches. *Metabolomics* **2021**, *17* (9), 78. https://doi.org/10.1007/s11306-021-01828-w.

(3) Vermunt, L.; Sikkes, S. A. M.; van den Hout, A.; et al. Duration of preclinical, prodromal, and dementia stages of Alzheimer's disease in relation to age, sex, and APOE genotype. Alzheimer's & Dementia **2019**, *15* (7), 888-898. https://doi.org/10.1016/j.jalz.2019.04.001.

(4) Qian, X.; Song, X.; Liu, X.; Chen, S.; Tang, H. Inflammatory Pathways in Alzheimer's Disease Mediated by Gut Microbiota. *Ageing Research Reviews* **2021**, *68*, 101317. https://doi.org/10.1016/j.arr.2021.101317.

(5) Heneka, M. T.; Carson, M. J.; El Khoury, J.; Landreth, G. E.; Brosseron, F.; Feinstein, D. L.; Jacobs, A. H.; Wyss-Coray, T.; Vitorica, J.; Ransohoff, R. M.; Herrup, K.; Frautschy, S. A.; Finsen, B.; Brown, G. C.; Verkhratsky, A.; Yamanaka, K.; Koistinaho, J.; Latz, E.; Halle, A.; Petzold, G. C.; Town, T.; Morgan, D.; Shinohara, M. L.; Perry, V. H.; Holmes, C.; Bazan, N. G.; Brooks, D. J.; Hunot, S.; Joseph, B.; Deigendesch, N.; Garaschuk, O.; Boddeke, E.; Dinarello, C. A.; Breitner, J. C.; Cole, G. M.; Golenbock, D. T.; Kummer, M. P. Neuroinflammation in Alzheimer's Disease. *Lancet Neurol* **2015**, *14* (4), 388–405. https://doi.org/10.1016/S1474-4422(15)70016-5.

(6) Mulak, A. Bile Acids as Key Modulators of the Brain-Gut-Microbiota Axis in Alzheimer's Disease. *J Alzheimers Dis* **2021**, *84* (2), 461–477. https://doi.org/10.3233/JAD-210608.

(7) Microbiota-Gut-Brain Axis in the Alzheimer's Disease Pathology - an Overview. *Neuroscience Research* **2022**, *181*, 17–21. https://doi.org/10.1016/j.neures.2022.05.003.

(8) Dhiman, K.; Blennow, K.; Zetterberg, H.; Martins, R. N.; Gupta, V. B. Cerebrospinal Fluid Biomarkers for Understanding Multiple Aspects of Alzheimer's Disease Pathogenesis. *Cell Mol Life Sci* **2019**, *76* (10), 1833–1863. https://doi.org/10.1007/s00018-019-03040-5.

(9) Mielke, M. M.; Syrjanen, J. A.; Blennow, K.; Zetterberg, H.; Vemuri, P.; Skoog, I.; Machulda, M. M.; Kremers, W. K.; Knopman, D. S.; Jack, C.; Petersen, R. C.; Kern, S. Plasma and CSF Neurofilament Light. *Neurology* **2019**, *93* (3), e252–e260. https://doi.org/10.1212/WNL.0000000000007767.

(10) Wishart, D. S.; Lewis, M. J.; Morrissey, J. A.; Flegel, M. D.; Jeroncic, K.; Xiong, Y.; Cheng, D.; Eisner, R.; Gautam, B.; Tzur, D.; Sawhney, S.; Bamforth, F.; Greiner, R.; Li, L. The Human Cerebrospinal Fluid Metabolome. *J Chromatogr B Analyt Technol Biomed Life Sci* **2008**, *871* (2), 164–173. https://doi.org/10.1016/j.jchromb.2008.05.001.

(11) *CSF Metabolome*. https://csfmetabolome.ca/ (accessed 2023-06-06).

(12) Schymanski, E. L.; Kondić, T.; Neumann, S.; Thiessen, P. A.; Zhang, J.; Bolton, E. E. Empowering Large Chemical Knowledge Bases for Exposomics: PubChemLite Meets MetFrag. *J Cheminform* **2021**, *13* (1), 19. https://doi.org/10.1186/s13321-021-00489-0.

(13) Bolton, E. E.; Wang, Y.; Thiessen, P. A.; Bryant, S. H. Chapter 12 - PubChem: Integrated Platform of Small Molecules and Biological Activities. In *Annual Reports in Computational Chemistry*; Wheeler, R. A., Spellmeyer, D. C., Eds.; Elsevier, 2008; Vol. 4, pp 217–241. https://doi.org/10.1016/S1574-1400(08)00012-1.

(14) Kim, S.; Chen, J.; Cheng, T.; Gindulyte, A.; He, J.; He, S.; Li, Q.; Shoemaker, B. A.; Thiessen, P. A.; Yu, B.; Zaslavsky, L.; Zhang, J.; Bolton, E. E. PubChem in 2021: New Data Content and Improved Web Interfaces. *Nucleic Acids Research* **2021**, *49* (D1), D1388–D1395. https://doi.org/10.1093/nar/gkaa971.

(15) Talavera Andújar, B.; Aurich, D.; Aho, V. T. E.; Singh, R. R.; Cheng, T.; Zaslavsky, L.; Bolton, E. E.; Mollenhauer, B.; Wilmes, P.; Schymanski, E. L. Studying the Parkinson's Disease Metabolome and Exposome in Biological Samples through Different Analytical and Cheminformatics Approaches: A Pilot Study. *Anal Bioanal Chem* **2022**. https://doi.org/validanti.

(16) Song, Z.; Wang, M.; Zhu, Z.; Tang, G.; Liu, Y.; Chai, Y. Optimization of Pretreatment Methods for Cerebrospinal Fluid Metabolomics Based on Ultrahigh Performance Liquid Chromatography/Mass Spectrometry. *Journal of Pharmaceutical and Biomedical Analysis* **2021**, *197*, 113938. https://doi.org/10.1016/j.jpba.2021.113938.

(17) Broadhurst, D.; Goodacre, R.; Reinke, S. N.; Kuligowski, J.; Wilson, I. D.; Lewis, M. R.; Dunn, W. B. Guidelines and Considerations for the Use of System Suitability and Quality Control Samples in Mass Spectrometry Assays Applied in Untargeted Clinical Metabolomic Studies. *Metabolomics* **2018**, *14* (6), 72. https://doi.org/10.1007/s11306-018-1367-3.

(18) Frigerio, G.; Moruzzi, C.; Mercadante, R.; Schymanski, E. L.; Fustinoni, S. Development and Application of an LC-MS/MS Untargeted Exposomics Method with a Separated Pooled Quality Control Strategy. *Molecules* **2022**, *27* (8), 2580. https://doi.org/10.3390/molecules27082580.

(19) Chambers, M. C.; Maclean, B.; Burke, R.; Amodei, D.; Ruderman, D. L.; Neumann, S.; Gatto, L.; Fischer, B.; Pratt, B.; Egertson, J.; Hoff, K.; Kessner, D.; Tasman, N.; Shulman,

N.; Frewen, B.; Baker, T. A.; Brusniak, M.-Y.; Paulse, C.; Creasy, D.; Flashner, L.; Kani, K.; Moulding, C.; Seymour, S. L.; Nuwaysir, L. M.; Lefebvre, B.; Kuhlmann, F.; Roark, J.; Rainer, P.; Detlev, S.; Hemenway, T.; Huhmer, A.; Langridge, J.; Connolly, B.; Chadick, T.; Holly, K.; Eckels, J.; Deutsch, E. W.; Moritz, R. L.; Katz, J. E.; Agus, D. B.; MacCoss, M.; Tabb, D. L.; Mallick, P. A Cross-Platform Toolkit for Mass Spectrometry and Proteomics. *Nat Biotechnol* **2012**, *30* (10), 918–920. https://doi.org/10.1038/nbt.2377.

(20) Tsugawa, H.; Cajka, T.; Kind, T.; Ma, Y.; Higgins, B.; Ikeda, K.; Kanazawa, M.; VanderGheynst, J.; Fiehn, O.; Arita, M. MS-DIAL: Data-Independent MS/MS Deconvolution for Comprehensive Metabolome Analysis. *Nat Methods* **2015**, *12* (6), 523–526. https://doi.org/10.1038/nmeth.3393.

(21) Tsugawa, H.; Kind, T.; Nakabayashi, R.; Yukihira, D.; Tanaka, W.; Cajka, T.; Saito, K.; Fiehn, O.; Arita, M. Hydrogen Rearrangement Rules: Computational MS/MS Fragmentation and Structure Elucidation Using MS-FINDER Software. *Anal. Chem.* **2016**, *88* (16), 7946–7958. https://doi.org/10.1021/acs.analchem.6b00770.

(22) Lai, Z.; Tsugawa, H.; Wohlgemuth, G.; Mehta, S.; Mueller, M.; Zheng, Y.; Ogiwara, A.; Meissen, J.; Showalter, M.; Takeuchi, K.; Kind, T.; Beal, P.; Arita, M.; Fiehn, O. Identifying Metabolites by Integrating Metabolome Databases with Mass Spectrometry Cheminformatics. *Nat Methods* **2018**, *15* (1), 53–56. https://doi.org/10.1038/nmeth.4512.

(23) Helmus, R.; ter Laak, T. L.; van Wezel, A. P.; de Voogt, P.; Schymanski, E. L. PatRoon: Open Source Software Platform for Environmental Mass Spectrometry Based Non-Target Screening. *Journal of Cheminformatics* **2021**, *13* (1), 1. https://doi.org/10.1186/s13321-020-00477-w.

(24) Helmus, R.; Velde, B. van de; Brunner, A. M.; Laak, T. L. ter; Wezel, A. P. van; Schymanski, E. L. PatRoon 2.0: Improved Non-Target Analysis Workflows Including Automated Transformation Product Screening. *Journal of Open Source Software* **2022**, *7* (71), 4029. https://doi.org/10.21105/joss.04029.

(25) *Environmental Cheminformatics / AD-CSF · GitLab*. GitLab. https://gitlab.lcsb.uni.lu/eci/AD-CSF (accessed 2023-06-12).

(26) Andújar, B. T.; Mary, A.; Cheng, T.; Zaslavsky, L.; Bolton, E. E.; Heneka, M. T.; Schymanski, E. L. PubChem Lists to Study the Exposome of Mild Cognitive Impairment and Alzheimer's Disease on Cerebrospinal Fluid, 2023. https://doi.org/10.5281/zenodo.8014420.

(27) Bolton, E.; Schymanski, E.; Kondic, T.; Thiessen, P.; Zhang, J. PubChemLite for Exposomics, 2020. https://doi.org/10.5281/zenodo.4183801.

(28) Schymanski, E. L.; Jeon, J.; Gulde, R.; Fenner, K.; Ruff, M.; Singer, H. P.; Hollender, J. Identifying Small Molecules via High Resolution Mass Spectrometry: Communicating Confidence. *Environ. Sci. Technol.* **2014**, *48* (4), 2097–2098. https://doi.org/10.1021/es5002105.

(29) Dodder, N.; Mullen, K. OrgMassSpecR: Organic Mass Spectrometry, 2017. https://CRAN.R-project.org/package=OrgMassSpecR (accessed 2022-08-01).

(30) Liao, W.-L.; Heo, G.-Y.; Dodder, N. G.; Pikuleva, I. A.; Turko, I. V. Optimizing the Conditions of a Multiple Reaction Monitoring Assay for Membrane Proteins: Quantification of Cytochrome P450 11A1 and Adrenodoxin Reductase in Bovine Adrenal Cortex and Retina. *Anal. Chem.* **2010**, *82* (13), 5760–5767. https://doi.org/10.1021/ac100811x.

(31) Hoh, E.; Dodder, N. G.; Lehotay, S. J.; Pangallo, K. C.; Reddy, C. M.; Maruya, K. A. Nontargeted Comprehensive Two-Dimensional Gas Chromatography/Time-of-Flight Mass

582 Spectrometry Method and Software for Inventorying Persistent and Bioaccumulative
583 Contaminants in Marine Environments. *Environ. Sci. Technol.* **2012**, *46* (15), 8001–8008.
584 https://doi.org/10.1021/es301139q.
585 (32) Chong, J.; Xia, J. Using MetaboAnalyst 4.0 for Metabolomics Data Analysis, Interpretation,
586 and Integration with Other Omics Data. In *Computational Methods and Data Analysis for*
587 *Metabolomics*; Li, S., Ed.; Methods in Molecular Biology; Springer US: New York, NY,
588 2020; pp 337–360. https://doi.org/10.1007/978-1-0716-0239-3_17.
589 (33) *MetaboAnalyst*. https://www.metaboanalyst.ca/ (accessed 2022-03-10).
590 (34) Xia, J.; Broadhurst, D. I.; Wilson, M.; Wishart, D. S. Translational Biomarker Discovery in
591 Clinical Metabolomics: An Introductory Tutorial. *Metabolomics* **2013**, *9* (2), 280–299.
592 https://doi.org/10.1007/s11306-012-0482-9.
593 (35) Ibáñez, C.; Simó, C.; Martín-Álvarez, P. J.; Kivipelto, M.; Winblad, B.; Cedazo-Mínguez,
594 A.; Cifuentes, A. *Toward a Predictive Model of Alzheimer's Disease Progression Using*
595 *Capillary Electrophoresis–Mass Spectrometry Metabolomics*. ACS Publications.
596 https://doi.org/10.1021/ac301243k.
597 (36) Xie, K.; Qin, Q.; Long, Z.; Yang, Y.; Peng, C.; Xi, C.; Li, L.; Wu, Z.; Daria, V.; Zhao, Y.;
598 Wang, F.; Wang, M. High-Throughput Metabolomics for Discovering Potential Biomarkers
599 and Identifying Metabolic Mechanisms in Aging and Alzheimer's Disease. *Front Cell Dev*
600 *Biol* **2021**, *9*, 602887. https://doi.org/10.3389/fcell.2021.602887.
601 (37) van der Velpen, V.; Teav, T.; Gallart-Ayala, H.; Mehl, F.; Konz, I.; Clark, C.; Oikonomidi,
602 A.; Peyratout, G.; Henry, H.; Delorenzi, M.; Ivanisevic, J.; Popp, J. Systemic and Central
603 Nervous System Metabolic Alterations in Alzheimer's Disease. *Alz Res Therapy* **2019**, *11*
604 (1), 93. https://doi.org/10.1186/s13195-019-0551-7.

(38) Nielsen, J. E.; Maltesen, R. G.; Havelund, J. F.; Færgeman, N. J.; Gotfredsen, C. H.; Vestergård, K.; Kristensen, S. R.; Pedersen, S. Characterising Alzheimer's Disease through Integrative NMR- and LC-MS-Based Metabolomics. *Metabolism Open* **2021**, *12*, 100125. https://doi.org/10.1016/j.metop.2021.100125.

(39) Pingle, S. C.; Lin, F.; Anekoji, M.S.; et al. Exploring the role of cerebrospinal fluid as analyte in neurologic disorders. *Future Science OA*, **2023,** *9* (4). https://doi.org/10.2144/fsoa-2023-0006.

(40) Human Gray and White Matter Metabolomics to Differentiate APOE and Stage Dependent Changes in Alzheimer's Disease. *Journal of Cellular Immunology* **2021**, *3* (6). https://doi.org/10.33696/immunology.3.123.

(41) LeWitt, P. A.; Li, J.; Lu, M.; Beach, T. G.; Adler, C. H.; Guo, L.; Consortium, the A. P. D. 3-Hydroxykynurenine and Other Parkinson's Disease Biomarkers Discovered by Metabolomic Analysis. *Movement Disorders* **2013**, *28* (12), 1653–1660. https://doi.org/10.1002/mds.25555.

(42) Sun, J.; Zhang, Y.; Kong, Y.; Ye, T.; Yu, Q.; Kumaran Satyanarayanan, S.; Su, K.-P.; Liu, J. Microbiota-Derived Metabolite Indoles Induced Aryl Hydrocarbon Receptor Activation and Inhibited Neuroinflammation in APP/PS1 Mice. *Brain, Behavior, and Immunity* **2022**, *106*, 76–88. https://doi.org/10.1016/j.bbi.2022.08.003.

(43) Wu, L.; Han, Y.; Zheng, Z.; Peng, G.; Liu, P.; Yue, S.; Zhu, S.; Chen, J.; Lv, H.; Shao, L.; Sheng, Y.; Wang, Y.; Li, L.; Li, L.; Wang, B. Altered Gut Microbial Metabolites in Amnestic Mild Cognitive Impairment and Alzheimer's Disease: Signals in Host-Microbe Interplay. *Nutrients* **2021**, *13* (1), 228. https://doi.org/10.3390/nu13010228.

(44) Lin, Y.-T.; Wu, P.-H.; Lee, H.-H.; Mubanga, M.; Chen, C.-S.; Kuo, M.-C.; Chiu, Y.-W.; Kuo, P.-L.; Hwang, S.-J. Indole-3 Acetic Acid Increased Risk of Impaired Cognitive Function in Patients Receiving Hemodialysis. *NeuroToxicology* **2019**, *73*, 85–91. https://doi.org/10.1016/j.neuro.2019.02.019.

(45) Mu, W.; Yang, Y.; Jia, J.; Zhang, T.; Jiang, B. Production of 4-Hydroxyphenyllactic Acid by Lactobacillus Sp. SK007 Fermentation. *J Biosci Bioeng* **2010**, *109* (4), 369–371. https://doi.org/10.1016/j.jbiosc.2009.10.005.

(46) Kori, M.; Aydın, B.; Unal, S.; Arga, K. Y.; Kazan, D. Metabolic Biomarkers and Neurodegeneration: A Pathway Enrichment Analysis of Alzheimer's Disease, Parkinson's Disease, and Amyotrophic Lateral Sclerosis. *OMICS: A Journal of Integrative Biology* **2016**, *20* (11), 645–661. https://doi.org/10.1089/omi.2016.0106.

(47) Lin, C.; Zhao, S.; Zhu, Y.; Fan, Z.; Wang, J.; Zhang, B.; Chen, Y. Microbiota-Gut-Brain Axis and Toll-like Receptors in Alzheimer's Disease. *Computational and Structural Biotechnology Journal* **2019**, *17*, 1309–1317. https://doi.org/10.1016/j.csbj.2019.09.008.

(48) Jensen, N. J.; Wodschow, H. Z.; Nilsson, M.; Rungby, J. Effects of Ketone Bodies on Brain Metabolism and Function in Neurodegenerative Diseases. *International Journal of Molecular Sciences* **2020**, *21* (22), 8767. https://doi.org/10.3390/ijms21228767.

(49) Shippy, D. C.; Wilhelm, C.; Viharkumar, P. A.; Raife, T. J.; Ulland, T. K. β-Hydroxybutyrate Inhibits Inflammasome Activation to Attenuate Alzheimer's Disease Pathology. *Journal of Neuroinflammation* **2020**, *17* (1), 280. https://doi.org/10.1186/s12974-020-01948-5.

(50) Reger, M. A.; Henderson, S. T.; Hale, C.; Cholerton, B.; Baker, L. D.; Watson, G. S.; Hyde, K.; Chapman, D.; Craft, S. Effects of Beta-Hydroxybutyrate on Cognition in Memory-

649 Impaired Adults. *Neurobiol Aging* **2004**, *25* (3), 311–314. https://doi.org/10.1016/S0197-
650 4580(03)00087-3.
651 (51) Leclercq, S.; Le Roy, T.; Furgiuele, S.; Coste, V.; Bindels, L. B.; Leyrolle, Q.; Neyrinck, A.
652 M.; Quoilin, C.; Amadieu, C.; Petit, G.; Dricot, L.; Tagliatti, V.; Cani, P. D.; Verbeke, K.;
653 Colet, J.-M.; Stärkel, P.; de Timary, P.; Delzenne, N. M. Gut Microbiota-Induced Changes
654 in β-Hydroxybutyrate Metabolism Are Linked to Altered Sociability and Depression in
655 Alcohol Use Disorder. *Cell Reports* **2020**, *33* (2), 108238.
656 https://doi.org/10.1016/j.celrep.2020.108238.
657 (52) Esteve, C.; Jones, E. A.; Kell, D. B.; Boutin, H.; McDonnell, L. A. Mass Spectrometry
658 Imaging Shows Major Derangements in Neurogranin and in Purine Metabolism in the Triple-
659 Knockout 3×Tg Alzheimer Mouse Model. *Biochimica et Biophysica Acta (BBA) - Proteins*
660 *and Proteomics* **2017**, *1865* (7), 747–754. https://doi.org/10.1016/j.bbapap.2017.04.002.
661 (53) Yilmaz, A.; Ugur, Z.; Bisgin, H.; Akyol, S.; Bahado-Singh, R.; Wilson, G.; Imam, K.;
662 Maddens, M. E.; Graham, S. F. Targeted Metabolic Profiling of Urine Highlights a Potential
663 Biomarker Panel for the Diagnosis of Alzheimer's Disease and Mild Cognitive Impairment:
664 A Pilot Study. *Metabolites* **2020**, *10* (9), 357. https://doi.org/10.3390/metabo10090357.
665 (54) Wang, G.; Zhou, Y.; Huang, F.-J.; Tang, H.-D.; Xu, X.-H.; Liu, J.-J.; Wang, Y.; Deng, Y.-
666 L.; Ren, R.-J.; Xu, W.; Ma, J.-F.; Zhang, Y.-N.; Zhao, A.-H.; Chen, S.-D.; Jia, W. Plasma
667 Metabolite Profiles of Alzheimer's Disease and Mild Cognitive Impairment. *J. Proteome*
668 *Res.* **2014**, *13* (5), 2649–2658. https://doi.org/10.1021/pr5000895.
669 (55) Park, S. J.; Lee, J.; Lee, S.; Lim, S.; Noh, J.; Cho, S. Y.; Ha, J.; Kim, H.; Kim, C.; Park, S.;
670 Lee, D. Y.; Kim, E. Exposure of Ultrafine Particulate Matter Causes Glutathione Redox
671 Imbalance in the Hippocampus: A Neurometabolic Susceptibility to Alzheimer's Pathology.

672 *Science of The Total Environment* **2020**, *718*, 137267.
673 https://doi.org/10.1016/j.scitotenv.2020.137267.
674 (56) Sun, Q.; Weinger, J. G.; Mao, F.; Liu, G. Regulation of structural and functional synapse
675 density by L-threonate through modulation of intraneuronal magnesium concentration.
676 *Neuropharmacology* **2016** *108*, 426-439. https://doi.org/10.1016/j.neuropharm.2016.05.006.
677 (57) Trezzi, J.-P.; Galozzi, S.; Jaeger, C.; Barkovits, K.; Brockmann, K.; Maetzler, W.; Berg, D.;
678 Marcus, K.; Betsou, F.; Hiller, K.; Mollenhauer, B. Distinct Metabolomic Signature in
679 Cerebrospinal Fluid in Early Parkinson's Disease: Early Parkinson'S CSF Metabolic
680 Signature. *Mov Disord.* **2017**, *32* (10), 1401–1408. https://doi.org/10.1002/mds.27132.
681 (58) Beukema, M.; Faas, M. M.; de Vos, P. The Effects of Different Dietary Fiber Pectin
682 Structures on the Gastrointestinal Immune Barrier: Impact via Gut Microbiota and Direct
683 Effects on Immune Cells. *Exp Mol Med* **2020**, *52* (9), 1364–1376.
684 https://doi.org/10.1038/s12276-020-0449-2.
685 (59) Echeverria, V.; Zeitlin, R. Cotinine: A Potential New Therapeutic Agent against Alzheimer's
686 Disease. *CNS Neurosci Ther* **2012**, *18* (7), 517–523. https://doi.org/10.1111/j.1755-
687 5949.2012.00317.x.
688 (60) Patel, S.; Grizzell, J. A.; Holmes, R.; Zeitlin, R.; Solomon, R.; Sutton, T. L.; Rohani, A.;
689 Charry, L. C.; Iarkov, A.; Mori, T.; Echeverria Moran, V. Cotinine Halts the Advance of
690 Alzheimer's Disease-like Pathology and Associated Depressive-like Behavior in Tg6799
691 Mice. *Front Aging Neurosci* **2014**, *6*, 162. https://doi.org/10.3389/fnagi.2014.00162.
692
693